Singular vector filtering method for mitigation of disturbance enhancement in multichannel active noise control systems

Yongjie Zhuang [a], Xuchen Wang [b], and Yangfan Liu [a]
[a] Ray W. Herrick Laboratories, Purdue University, West Lafayette, IN 47907, USA. Email: yangfan@purdue.edu
[b] Academic building 1, 2/F, The Chinese University of Hong Kong, Sha Tin, Hong Kong SAR, 999077, China.

In the design of multichannel active noise control filters, the disturbance enhancement phenomenon will sometimes occur, i.e., the resulting sound is enhanced instead of being reduced in some frequency bands, if the control filter is designed to minimize the power of error signals in other frequency bands or across all frequencies. In previous work, a truncated singular value decomposition method was applied to the system autocorrelation matrix to mitigate the disturbance enhancement. Some small singular values and the associated singular vectors are removed, if they are responsible for unwanted disturbance enhancement in some frequency bands. However, some of these removed singular vectors may still contribute to the noise control performance in other frequency bands, thus a direct truncation will degrade the noise control performance. In the present work, through an additional filtering process, the set of singular vectors that cause the disturbance enhancement are replaced by a set of new singular vectors whose frequency responses are attenuated in the frequency band where disturbance enhancement occurs, while the frequency responses in other frequency bands are unchanged. Compared with truncation approach, the proposed method can maintain the performance in the noise reduction bands, while mitigating the influence in disturbance enhancement bands.

Primary subject classification: 38.2; Secondary subject classification: 74.9

1 INTRODUCTION

In active noise control (ANC) systems, one or more control filters are designed to process the reference or error signals obtained by sensors such as microphones or accelerometers. The output signals of the control filters are used to drive secondary sources to produce an appropriate secondary sound field that can cancel or reduce the primary sound field at specified locations or regions. In the recent decades, because of the development of the computing devices, e.g., the Digital Signal Processor (DSP) and the Field-Programmable Gate Arrays (FPGA), ANC technologies were successfully applied to a wide range of applications, such as automobiles[1], headrests[2,3], and headphones[4,5].

One of the main focuses of ANC studies is the methods of designing appropriate control filters. The requirement for a control filter is to achieve good noise control performance and satisfy some practical criteria (stability, robustness, disturbance enhancement, etc.) at the same time. Among those criteria, the disturbance enhancement is particularly concerned in the current work. It requires that the control filter should have satisfactory noise control performance at the desired frequency bands without significantly enhancing the noise level in other frequency bands. The design of the ANC filters can be accomplished either in the time domain, or in the frequency domain[6]. For multichannel ANC systems, if filters are designed by minimizing the power of the resulting error sound, disturbance enhancement phenomenon will sometimes occur[7-10]. Different treatments for this disturbance enhancement phenomenon can be found in previous works, for example, the disturbance enhancement is constrained by adding enhancement constraints at each frequency band in the frequency domain to formulate an optimization problem[1,3,8,9]. Although this frequency-domain method is convenient in formulating the optimization problem, the computational complexity to solve the constrained optimization problem is significant, especially when the numbers of filter channels and coefficients are large. The enhancement bound can be also applied to the time-domain methods by introducing an adjustable penalty (or regularization) parameter into the formulation[10,11]. However, this penalty will usually affect the entire frequency band and sacrifice the noise control performance significantly, especially for the frequency band where no enhancement phenomenon occurs[6,12].

Recently, Liu et al. demonstrated that a singular value decomposition (SVD) based method can be used to extract independent sound field components[13]. Inspired by that work, Wang et al. proposed another time-domain treatment for disturbance enhancement where a truncated SVD method is applied[7]. SVD was firstly applied to the auto-correlation matrix of filtered-reference signals, and the singular values and singular vectors that contribute to the enhancement phenomenon were removed to mitigate the disturbance enhancement. Their results showed that this method can effectively mitigate the enhancement phenomenon. However, some of the removed singular values and singular vectors, although responsible for enhancement in certain frequency bands, may contribute to the noise control performance in other desired frequency bands. Thus, such a direct truncation will affect the noise control performance. To further reduce this effect, a filtering method is proposed in the present work. Instead of a direct truncation, a filtering process was introduced to replace the singular vectors contributing to the disturbance enhancement by a set of new singular vectors whose frequency responses are attenuated in the frequency band where disturbance enhancement occurs, while the frequency responses in other frequency bands are unchanged. Compared with truncation method, the proposed method can reduce the impact on the noise control performance at desired frequency bands and, at the same time, mitigate the disturbance enhancement phenomenon.

The paper is organized as follows, in Section 2, the theory related to the proposed filtering method is introduced; in Section 3, the simulation results of this filtering method are presented and compared with the direct truncation method; concluding comments are summarized in Section 4.

2 THEORY

In the current work, the proposed method is described in the context of a multichannel feedforward ANC system. Because for a feedback ANC system, if the internal model control (IMC) structure is used, the proposed method can be applied in a similar way. The only difference is that the error sensors would be also treated as reference sensors, and the acoustical feedback path is the same as the path from secondary sources to error sensors[1,6,14]. In this section, the typical algorithm for calculating the coefficients of the optimal control filters, regularization method, and the truncated singular value decomposition method are reviewed first, then the singular vector filtering method is described. In the current work, non-adaptive filter design is considered which is used in a wide range of current ANC applications, e.g., the commercial digital ANC headphones[15].

2.1 Traditional algorithm for optimal filter design

A multiple-input-multiple-output (MIMO) ANC system includes N_r reference sensors, N_s control sources, and N_e error sensors, The system block diagram of a typical MIMO ANC feedforward controller is shown in Figure 1, which is similar to the block diagram in Wang et al.'s work[7]. Elements in vector $\vec{\boldsymbol{p}}(n)$ are the reference signals measured by the reference sensors. When the ANC system is activated, it includes both the primary noise signals $\vec{\boldsymbol{x}}(n)$, representing the noise from the primary sources at the reference sensor locations, and the signals from secondary sources at the same reference sensor locations. $\vec{\boldsymbol{y}}(n)$ denotes the outputs of the controller, which are also the driving signals for secondary sources. $\vec{\boldsymbol{e}}(n)$ denotes the error signals measured at error sensor locations, which includes the disturbance signals $\vec{\boldsymbol{d}}(n)$ from the primary sources and the anti-noise signals from secondary sources. $\boldsymbol{G_s}$ is the acoustic feedback path from secondary sources to the reference sensors. To cancel influence of the acoustic feedback path, an internal model control (IMC) structure is used[1,3,14]. $\widehat{\boldsymbol{G}}_{\boldsymbol{s}}$ in the controller $\mathbf{H}$ is the estimate of the acoustic feedback path. In the current work, it is assumed that $\widehat{\boldsymbol{G}}_{\boldsymbol{s}} = \boldsymbol{G_s}$, so the estimate of noise signals $\hat{\vec{\boldsymbol{x}}}(n) = \vec{\boldsymbol{x}}(n)$. $\boldsymbol{G_e}$ is the secondary path from secondary sources to the error sensors. $\boldsymbol{W}$ denotes the $N_s \times N_r$ multichannel control filters. In the current work, each channel in the controller is an FIR filter with N_t coefficients.

The conventional method to calculate control parameters is to minimize the power of the error signals, $\vec{\boldsymbol{e}}(n)$, when ANC system is activated. The cost function of this optimization problem can be expressed as[6,7]:

$$E[\vec{\boldsymbol{e}}^T(n)\,\vec{\boldsymbol{e}}(n)] = \vec{\boldsymbol{w}}^T\boldsymbol{A}\vec{\boldsymbol{w}} + 2\vec{\boldsymbol{w}}^T\vec{\boldsymbol{b}} + c, \tag{1}$$

where,

$$\boldsymbol{A} = \mathrm{E}[\boldsymbol{R}^{\mathrm{T}}(n)\,\boldsymbol{R}(n)], \qquad \vec{\boldsymbol{b}} = \mathrm{E}\left[\boldsymbol{R}^{\mathrm{T}}(n)\,\vec{\boldsymbol{d}}(n)\right], \qquad c = \mathrm{E}\left[\vec{\boldsymbol{d}}^{\mathrm{T}}(n)\,\vec{\boldsymbol{d}}(n)\right],$$

$$\vec{\boldsymbol{w}} = \left[w_{1,1,0}, w_{1,2,0}, \dots, w_{1,N_r,0}, \dots, w_{N_s,N_r,0}, \dots, w_{N_s,N_r,N_t-1}\right]^{\mathrm{T}},$$

$$\boldsymbol{R}(n) = \begin{bmatrix} \vec{\boldsymbol{r}}_1^{\mathrm{T}}(n) & \vec{\boldsymbol{r}}_1^{\mathrm{T}}(n-1) & \cdots & \vec{\boldsymbol{r}}_1^{\mathrm{T}}(n-N_t+1) \\ \vec{\boldsymbol{r}}_2^{\mathrm{T}}(n) & \vec{\boldsymbol{r}}_2^{\mathrm{T}}(n-1) & \cdots & \vec{\boldsymbol{r}}_2^{\mathrm{T}}(n-N_t+1) \\ \vdots & \vdots & \ddots & \vdots \\ \vec{\boldsymbol{r}}_{N_e}^{\mathrm{T}}(n) & \vec{\boldsymbol{r}}_{N_e}^{\mathrm{T}}(n-1) & \cdots & \vec{\boldsymbol{r}}_{N_e}^{\mathrm{T}}(n-N_t+1) \end{bmatrix},$$

$$\vec{\boldsymbol{r}}_q(n) = \left[r_{q,1,1}(n), r_{q,1,2}(n), \dots, r_{q,1,N_r}(n), r_{q,2,1}(n), \dots, r_{q,N_r,N_t}(n)\right]^{\mathrm{T}},$$

$$r_{q,m,l}(n) = \textstyle\sum_{i=0}^{I-1} g_{q,m,j} x_l(n-j) \;,$$

where $g_{q,m,j}$ denotes the *j*-th coefficient of the FIR filter model of the component in $\boldsymbol{G_e}$ that corresponds to the *m*-th input and *q*-th output; $x_l(n)$ is the *l*-th element of $\vec{\boldsymbol{x}}(n)$. The optimal solution is[6,7]:

$$\vec{\boldsymbol{w}}_{opt} = -\boldsymbol{A}^{-1}\vec{\boldsymbol{b}} \;. \tag{2}$$

When the matrix $\boldsymbol{A}$ is near singular or the robust filter design is desired, Equation (2) can be modified by introducing a positive regularization parameter β:

$$\vec{\boldsymbol{w}}_{reg} = -(\boldsymbol{A} + \beta I)^{-1}\vec{\boldsymbol{b}} \;, \tag{3}$$

where the matrix $\boldsymbol{I}$ is an identity matrix. Equation (3) gives a regularized solution of the optimal filter coefficients (sometimes referred to as the robust filter design). If the regularization parameter β is chosen to be large enough, it is obvious that the designed filter $\vec{\boldsymbol{w}}_{reg}$ will have small response and thus, less likely to have disturbance enhancement.

2.2 Singular vector filtering method for mitigating disturbance enhancement

To investigate the disturbance enhancement phenomenon resulting from the mutual correlation of multichannel reference signals, Wang et al. applied SVD to the auto-correlation matrix $\boldsymbol{A}$ [7], which results in:

$$\boldsymbol{A} = \boldsymbol{U\Sigma U}^T = \begin{bmatrix}\vec{\boldsymbol{u}}_1 & \cdots & \vec{\boldsymbol{u}}_{N_rN_sN_t}\end{bmatrix}\begin{bmatrix}\boldsymbol{\sigma}_1 & \cdots & 0\\ \vdots & \ddots & \vdots\\ 0 & \cdots & \boldsymbol{\sigma}_{N_rN_sN_t}\end{bmatrix}\begin{bmatrix}\vec{\boldsymbol{u}}_1^T\\ \vdots\\ \vec{\boldsymbol{u}}_{N_rN_sN_t}^T\end{bmatrix}, \tag{4}$$

$$\vec{\boldsymbol{w}}_{opt} = -\sum_{k=1}^{N_rN_sN_t} \boldsymbol{\sigma}_k^{-1}\langle\vec{\boldsymbol{u}}_k, \vec{\boldsymbol{b}}\rangle\,\vec{\boldsymbol{u}}_k \ , \tag{5}$$

where < > denotes the inner product of two vectors. The optimal filter $\vec{\boldsymbol{w}}_{opt}$ can be considered as a linear combination of the singular vectors, $\vec{\boldsymbol{u}}_k$, each of which represents a MIMO FIR filter with N_r outputs, N_s inputs, and N_t filter coefficients. Sometimes there will be some very large value of $\boldsymbol{\sigma}_k^{-1}\langle\vec{\boldsymbol{u}}_k, \vec{\boldsymbol{b}}\rangle$, which then cause the disturbance enhancement[7]. To mitigate this disturbance enhancement, Wang et al. truncated the singular values and the associated singular vectors, after some index l, to form a modified filter[7]:

$$\vec{\boldsymbol{w}}_0 = -\sum_{k=1}^{l} \boldsymbol{\sigma}_k^{-1}\langle\vec{\boldsymbol{u}}_k, \vec{\boldsymbol{b}}\rangle\,\vec{\boldsymbol{u}}_k \ . \tag{6}$$

Then $\vec{\boldsymbol{w}}_0$ will be used to replace $\vec{\boldsymbol{w}}_{opt}$ as the control filter. It was demonstrated that this method could mitigate the enhancement if l is chosen appropriately. However, the discarded singular values and vectors also contribute to the noise control performance at other frequency bands, thus such a direct truncation will negatively affect the overall noise control performance.

To reduce this impact on the noise control performance in desired frequency bands, a filtering method, instead of truncation, is proposed. Firstly, the original singular vector representation of the optimal filter, Equation (5), can be divided as two groups:

$$\vec{\boldsymbol{w}}_{opt} = \vec{\boldsymbol{w}}_0 + \sum_{k=l+1}^{m} \vec{\boldsymbol{w}}_k + \sum_{k=m+1}^{N_rN_sN_t} \vec{\boldsymbol{w}}_k \ , \tag{7}$$

where $\vec{\boldsymbol{w}}_0$ is defined in Equation (6), which are the singular vectors with no enhancement contributions, and $\vec{\boldsymbol{w}}_k$ is the component in the subspace spanned by the singular vector contributing to enhancement in certain bands (i.e., the component that is removed in Wang, et al.'s work), which is expressed as:

$$\vec{\boldsymbol{w}}_k = -\boldsymbol{\sigma}_k^{-1}\langle\vec{\boldsymbol{u}}_k, \vec{\boldsymbol{b}}\rangle\,\vec{\boldsymbol{u}}_k = \left[w_{k,1,1,0}, w_{k,1,2,0}, \dots, w_{k,1,N_r,0}, \dots, w_{k,N_s,N_r,0}, \dots, w_{k,N_s,N_r,N_t-1}\right]^T. \tag{8}$$

The index m in Equation (7) suggests that from index $l+1$ to m, the singular vector contains responses that contribute to both the disturbance enhancement and the noise control performance while after index m, the singular vector contains responses that cause the disturbance enhancement only (thus, they should be always truncated). It is noted that $\vec{\boldsymbol{w}}_k$ can be rearranged to an $N_s \times N_r$ filters $\vec{\boldsymbol{w}}_{k,i,j}$ with a filter length of N_t for each input-output channel pair. The frequency response of $\vec{\boldsymbol{w}}_{k,i,j}$ can be evaluated appropriately at N_f frequency points:

$$\vec{\boldsymbol{W}}_{k,i,j} = \boldsymbol{F}_z\vec{\boldsymbol{w}}_{k,i,j} \ , \tag{9}$$

where,

$$\boldsymbol{F}_z = \begin{bmatrix} 1 & \mathrm{e}^{-j2\pi f_1 \frac{1}{f_s}} & \cdots & \mathrm{e}^{-j2\pi f_1 \frac{N_t-1}{f_s}} \\ 1 & \mathrm{e}^{-j2\pi f_2 \frac{1}{f_s}} & \cdots & \mathrm{e}^{-j2\pi f_2 \frac{N_t-1}{f_s}} \\ \vdots & \vdots & \ddots & \vdots \\ 1 & \mathrm{e}^{-j2\pi f_{N_f} \frac{1}{f_s}} & \cdots & \mathrm{e}^{-j2\pi f_{N_f} \frac{N_t-1}{f_s}} \end{bmatrix},$$

f_k is the k-th frequency; i and j represent the indices of different input and output channels of the multichannel filter $\vec{\boldsymbol{w}}_k$; f_s is the sampling frequency. As mentioned earlier, although $\vec{\boldsymbol{w}}_k$ is responsible for the enhancement phenomenon in some frequency bands, it also contributes to active noise control performance in other bands, thus a direct removal of $\vec{\boldsymbol{w}}_k$, as in the work of Wang et al., will inevitably sacrifice the noise control performance. It is proposed in the current work that a suitably designed band-stop filter can be applied to each channel pair of $\vec{\boldsymbol{W}}_{k,i,j}$ to obtain a new filter, $\vec{\vec{\boldsymbol{W}}}_{k,i,j}$, such that the stopbands of the designed filter cover the frequency bands where disturbance enhancement phenomenon occurs if the original $\vec{\boldsymbol{W}}_{k,i,j}$ were used (see Figure 2 for an intuitive illustration. Note that Figure 2 is not presenting actual results but to illustrate the process.). In this way, $\vec{\vec{\boldsymbol{W}}}_{k,i,j}$ can be treated as a filtered version of $\vec{\boldsymbol{W}}_{k,i,j}$, thus the proposed method is referred to as singular vector filtering method. It is important to note that the band-stop filter used in the current work differs from conventional band-stop filters in that the filter used in the current work should produce no change in either magnitude or phase in the pass-band, whereas, conventional band stop filters usually do not involve this zero phase requirement in the pass-band. Thus, instead of using conventional band-stop filter design methods, the FIR filter coefficients (denoted as $\vec{\boldsymbol{v}}_{k,i,j}$) representing the filtered filter $\vec{\vec{\boldsymbol{W}}}_{k,i,j}$ with the same filter length as $\vec{\boldsymbol{W}}_{k,i,j}$ are obtained by solving the following optimization problem:

$$\vec{\boldsymbol{v}}_{k,i,j} = arg \min_{\vec{\boldsymbol{v}}_{k,i,j}} \left\| \boldsymbol{F}_z \vec{\boldsymbol{v}}_{k,i,j} - \vec{\vec{\boldsymbol{W}}}_{k,i,j} \right\|_2^2 = Re\{\boldsymbol{F}_z^H \boldsymbol{F}_z\}^{-\mathbf{1}} Re\left\{\boldsymbol{F}_z^H \vec{\vec{\boldsymbol{W}}}_{k,i,j}\right\}, \tag{10}$$

where Re denotes taking the real part, and H denotes the complex conjugate transpose operation. Since the frequency response $\vec{\vec{\boldsymbol{W}}}_{k,i,j}$ is small in the frequency bands where disturbance enhancement occurs and is the same as $\vec{\boldsymbol{W}}_{k,i,j}$ in other frequency bands, the filter $\vec{\boldsymbol{v}}_{k,i,j}$ will not have enhancement problem while preserve the noise control performance at other frequency bands as much as possible. Also, the $\vec{\boldsymbol{v}}_{k,i,j}$ obtained from optimization will not have the impractical sharp transition in the frequency responses as $\vec{\vec{\boldsymbol{W}}}_{k,i,j}$. Then, $\vec{\boldsymbol{v}}_{k,i,j}$ can be rearranged to get:

$$\vec{\boldsymbol{v}}_k = \left[v_{k,1,1,0}, v_{k,1,2,0}, \dots, v_{k,1,N_r,0}, \dots, v_{k,N_s,N_r,0}, \dots, v_{k,N_s,N_r,N_t-1}\right]^T. \tag{11}$$

Finally, the modified filter by singular vector filtering method is:

$$\vec{\boldsymbol{w}}_{mod1} = \vec{\boldsymbol{w}}_0 + \sum_{k=l+1}^{m} \vec{\boldsymbol{v}}_k \ , \tag{12}$$

where $\vec{\boldsymbol{w}}_{mod1}$ can be used to replace $\vec{\boldsymbol{w}}_{opt}$ as control filters for the active noise control system.

However, if $\vec{\boldsymbol{v}}_{k,i,j}$ is to be obtained separately for each i, j pair and for each index k, the optimization problem specified in Equation (10) will need to be solved for $N_r \times N_s \times (m-l)$ times, which involves a significant calculation effort if $N_r \times N_s \times m$ is large and l is small. This process can be simplified if $\vec{\boldsymbol{v}}_{k,i,j}$ are obtained after summation over k. In usual ANC practices, the frequency bands where disturbance enhancement occurs are found to be similar for each $\vec{\boldsymbol{W}}_{k,i,j}$, this suggests that the same band-stop filter can be applied to all $\vec{\boldsymbol{W}}_{k,i,j}$. Thus, in order to simplify the proposed filtering process, $\vec{\boldsymbol{w}}_{k,i,j}$ can be added first, then calculated for its frequency response:

$$\vec{\boldsymbol{W}}_{sum,i,j} = \boldsymbol{F}_z\left(\sum_{k=l+1}^{m} \vec{\boldsymbol{w}}_{k,i,j}\right). \tag{13}$$

Then frequency responses of those band-stop filters can be multiplied to the frequency response $\vec{\boldsymbol{W}}_{sum,i,j}$ to obtain $\vec{\widetilde{\boldsymbol{W}}}_{sum,i,j}$ such that the stopbands cover all the frequency bands where disturbance enhancement occurs (a similar process as that in Figure 2). Then the second term in Equation (12) can be calculated by a single step:

$$\vec{\boldsymbol{v}}_{sum,i,j} = arg \min_{\vec{\boldsymbol{v}}_{sum,i,j}} \left\| \boldsymbol{F}_z \vec{\boldsymbol{v}}_{sum,i,j} - \vec{\widetilde{\boldsymbol{W}}}_{sum,i,j} \right\|_2^2 = Re\{\boldsymbol{F}_z^H \boldsymbol{F}_z\}^{-1} Re\left\{\boldsymbol{F}_z^H \vec{\widetilde{\boldsymbol{W}}}_{sum,i,j}\right\}, \tag{14}$$

Using similar way in Equation (11) to rearrange $\vec{\boldsymbol{v}}_{sum,i,j}$ to get $\vec{\boldsymbol{v}}_{sum}$, then we have:

$$\vec{\boldsymbol{w}}_{mod2} = \vec{\boldsymbol{w}}_0 + \vec{\boldsymbol{v}}_{sum} \ , \tag{15}$$

where $\vec{\boldsymbol{w}}_{mod2}$ can be used to replace $\vec{\boldsymbol{w}}_{opt}$ as control filters. Using this method, i.e., filtering after summation, the Equation (14) only need to be computed for $N_r \times N_s$ times, which is much more computationally efficient than repetitively solving Equation (10) for different k indices. In the next section, results obtained by filtering after summation, i.e., Equation (15), and by filtering separately, i.e., Equation (12), will also be compared.

3 RESULTS

3.1 The experimental setup for acquiring required data

In the present work, simulation results were based on experimental data obtained from an experiment of a multi-channel feedforward ANC system for a headrest application in room environment, which is similar to the works of Wang et al. [7] and is shown in Figure 3. The ANC system used in the current simulation work consists of two reference microphones (i.e., $N_r = 2$), four error microphones (i.e., $N_e = 4$), two loudspeakers as secondary sources (i.e., $N_s = 2$), and two loudspeakers as primary noise sources. All microphones and speakers were placed symmetrically at both sides with respect to the dummy's head. When acquiring measurement data, the sampling rate of data acquisition system was set to be 24000 Hz with proper anti-aliasing filters. Two million sampling points (around 83 seconds) for each channel were acquired for calculating the correlation matrices. A hamming window of 24000 points is used for averaging with fifty percent overlapping (165 times averages) to compute the cross spectral matrix first. Then the correlation function is computed by inverse Fourier transform on corresponding terms in the cross spectral matrix. After measuring the secondary path responses, appropriate delay is added into the secondary path representing the total time delay in the electronic controller due to analog-to-digital converter, processing time, DC removal high pass filters, anti-aliasing and reconstruction filters. The sampling frequency of control filter was chosen to be 2000 Hz. The length of FIR filter for each channel is 128. Thus, there are 512 singular vectors in total after decomposing matrix $\boldsymbol{A}$.

3.2 Comparison of truncated SVD method and singular vector filtering method

The results presented in the current work are based on off-line simulations using experimentally measured data in the setup described above. The frequency responses of singular vectors are shown in Figure 4. Because there are two reference microphones and two control speakers, i.e., 4 channel pairs, there are in total 4 plots denoted from (a) to (d) in Figure 4. The singular vector index denotes the index for singular vectors associated with singular values sorted from large to small. The comparison of simulated sound pressure averaged among the error microphones for different controller design methods is shown in Figure 5. “ANC OFF” denotes the sound pressure power spectral density function (PSD) of original disturbance signals averaged among all the error microphones. The “Normalized SPL” is the dB scale (i.e., ten times the logarithm) of the ratio of error microphone averaged sound PSD when different controllers are in operation to the PSD firstly averaged over error microphones and then averaged over the whole frequency band when "ANC OFF". “Original optimal filter” denotes the result when ANC system is operating using $\vec{\boldsymbol{w}}_{opt}$ in Equation (2). “Truncated SVD method” denotes the result when ANC system is operating using $\vec{\boldsymbol{w}}_0$ in Equation (6). “Singular vector filtering” denotes the result when ANC system is operating using $\vec{\boldsymbol{w}}_{mod2}$ in Equation (15).

From Figure 5, by comparing “Original optimal filter” and “ANC OFF”, it is obvious that the disturbance enhancement phenomenon occurs at frequencies below 200 Hz. It is also noted that the original optimal filter can result in a reasonable ANC performance above 200 Hz. From Figure 4, the singular vectors above index 120 are considered to have large magnitude of frequency responses where disturbance enhancement occurs as shown in Figure 5 (i.e., below 200 Hz). So, the stopbands of band-stop filters used in the current work are specified to cover those three frequency ranges and l in Equation (6) is chosen to be 120. The index m is chosen to be 350 because some trials show that the responses above index 350 only contribute to disturbance enhancement. On the other hand, frequency responses corresponding to singular vectors (shown in Figure 4) indeed shows that, although the singular vectors from index 120 to 350 have strong responses below 200 Hz where disturbance enhancement occurs, some of them also have strong responses at frequency range above 200 Hz, which may be important contributors to the noise control performance. Thus, truncating them will negatively affect the noise control performance at those frequency ranges.

After applying truncated SVD method and singular vector filtering method, from Figure 5, it can be seen that both “Truncated SVD method” and “Singular vector filtering method” can mitigate the disturbance enhancement effectively. Although the singular vector filtering method also sacrifices certain level of noise control performance compared with the original optimal filter, this proposed method can still have a better noise control performance compared with truncated SVD method in the frequency bands where no enhancement occurs when the original optimal filter is used (in this example, 400 Hz to 800 Hz).

To better demonstrate the proposed singular vector filtering method, Figure 6 shows the frequency responses of sum of singular vectors from index 120 to index 350. “Original responses” denotes the frequency responses of those singular vectors from the original optimal filter $\vec{\boldsymbol{w}}_{opt}$, i.e., the $\vec{\boldsymbol{W}}_{sum,i,j}$;

"Target responses" denotes $\vec{\overline{\boldsymbol{W}}}_{sum,i,j}$, the direct modified frequency responses; "Filtered responses" denotes the final frequency responses after fitting, i.e., the frequency responses of $\vec{\boldsymbol{v}}_{sum}$. From Figure 6, it can be observed that the proposed method can fit a $\vec{\boldsymbol{v}}_{sum}$ that closely matches the original frequency responses at frequency band where no disturbance enhancement occurs, i.e., above 200 Hz, while attenuate the frequency responses below 200 Hz where disturbance enhancement occurs.

3.3 Comparison of regularization method and singular vector filtering method

As mentioned in the previous sections, regularization method, i.e., Equation (3) , can also mitigate disturbance enhancement. Thus, the comparison of performance of regularization method and singular vector filtering method is shown in Figure 7. The regularization parameter is tuned and adjusted such that it is around the minimum value that can mitigate the disturbance enhancement to desired level. From Figure 7, we can see that the proposed singular vector filtering method can have a better noise control performance compared with the regularization method.

3.4 Comparison of two different singular vector filtering methods

The performance of two different singular vector filtering methods mentioned in Section 2 are compared in Figure 8. "Singular vector filtering method 1" denotes the result when ANC system is operating using $\vec{\boldsymbol{w}}_{mod1}$ in Equation (12), i.e., filtering each filter separately. "Singular vector filtering method 2" denotes the result when ANC system is operating using $\vec{\boldsymbol{w}}_{mod2}$ in Equation (15), i.e., filtering after summation. It can be seen that the performance has no obvious difference between these two methods. However, the calculation of $\vec{\boldsymbol{w}}_{mod2}$ is much more computationally efficient, so using the "Singular vector filtering method 2" is preferable in practice.

4 CONCLUDING COMMENTS

In the present work, a singular vector filtering method was proposed for ANC systems to mitigate the disturbance enhancement phenomenon. The proposed method firstly applies SVD to the auto-correlation matrix of filtered-reference signals. Then the singular vectors are divided into three groups. The group with larger singular values is unchanged, but the second group (the group with smaller singular values) is replaced by a new set of filters. Sometimes, for near singular autocorrelation matrix, extremely small singular values (form the third group) will be discarded. The new set of filters are obtained by filtering the filters represented by the singular vectors in the second group through properly designed band-stop filters with the stopbands covering the frequency bands where disturbance enhancement occurs. In this way, the enhancement phenomenon can be mitigated. The band-stop filters were not designed or implemented using conventional methods, instead, the coefficients of the new set of filters are obtained by a least-square match to the frequency response of the singular vectors in the second group with the responses in the specified stop-bands changed to small magnitudes.

The simulation results showed that the proposed singular vector filtering method can mitigate the disturbance enhancement as effectively as the truncated SVD method. Also, compared with truncated SVD method, the noise control performance can be better in other frequency ranges by using the singular vector filtering method. The analysis of this effect is also confirmed by checking the frequency responses of singular vectors for each channel. It was also demonstrated that the proposed singular vector filtering method can achieve better noise control performance compared with traditional regularization method. Also, two different singular vector filtering methods were compared, i.e., filtering each singular vector in the second group separately and filtering after summing up those singular vectors. The simulation results demonstrated that those two different approaches produce the same noise control performance, if the disturbance occurs at similar frequency bands for each singular vector. Thus, filtering after summation is preferable because it is more computationally efficient than filtering separately while having similar noise control performance.

So far, the proposed method is applied to non-adaptive filters. In the future, it may be converted into an adaptive algorithm by doing the calculation of eigenvalues and eigenvectors iteratively, and the minimization of Equation (14), i.e., a least-square estimation, iteratively using recursive least square.

5 ACKNOWLEDGMENTS

The authors thank Beijing Ancsonic Technology Co. Ltd for providing financial support for the present work. The author would also like to thank the anonymous reviewer for the valuable revision suggestions.

6 REFERENCES

1. J. Cheer and S. J. Elliott, "Multichannel control systems for the attenuation of interior road noise in vehicles," *Mechanical Systems and Signal Processing,* vol. 60, pp. 753--769, 2015.

2. Y. Liu and J. Liu, "The Stochastic Domain Design of a Real-Time Controller for an Active Noise Control Headrest based on Finite Element Analysis," *INTER-NOISE and NOISE-CON Congress and Conference Proceedings,* vol. 255, pp. 488--499, 2017.

3. B. Rafaely and S. J. Elliott, "H2 / H_infty active control of sound in a headrest: design and implementation," *IEEE Transactions on control systems technology,* vol. 7, pp. 79-84, 1999.

4. S. M. Kuo, S. Mitra and W.-S. Gan, "Active noise control system for headphone applications," *IEEE Transactions on Control Systems Technology,* vol. 14, no. 2, pp. 331-335, 2006.

5. M. Guldenschuh and R. De Callafon, "Detection of secondary-path irregularities in active noise control headphones," *IEEE/ACM transactions on audio, speech, and language processing,* vol. 22, no. 7, pp. 1148-1157, 2014.

6. S. Elliott, "Multichannel Control of Stochastic Disturbances," *Signal Processing for Active Control*, Academic Press, 2001, pp. 233-270.

7. X. Wang, Y. Liu and J. S. Bolton, "Truncated Singular Value Decomposition Method for Mitigating Unwanted Enhancement in Active Noise Control Systems," *INTER-NOISE and NOISE-CON Congress and Conference Proceedings*, 2018.

8. Y. Zhuang and Y. Liu, "Study on the Cone Programming Reformulation of Active Noise Control Filter Design in the Frequency Domain," *INTER-NOISE and NOISE-CON Congress and Conference Proceedings*, 2019.

9. Y. Zhuang and Y. Liu, "Development and Application of Dual Form Conic Formulation of Multichannel Active Noise Control Filter Design Problem in Frequency Domain," *INTER-NOISE and NOISE-CON Congress and Conference Proceedings*, 2020.

10. L. Wu, X. Qiu, and Y. Guo, "A generalized leaky FxLMS algorithm for tuning the waterbed effect of feedback active noise control systems," *Mechanical Systems and Signal Processing,* vol. 106, pp. 13--23, 2018.

11. F. An, Y. Cao, M. Wu, H. Sun, B. Liu, and J. Yang, "Robust Wiener controller design with acoustic feedback for active noise control systems," *The Journal of the Acoustical Society of America,* vol. 145, pp. EL291--EL296, 2019.

12. S. J. Elliott, C. C. Boucher and P. A. Nelson, "The behavior of a multiple channel active control system," *IEEE Transactions on signal processing,* vol. 40, no. 5, pp. 1041-1052, 1992.

13. Y. Liu, S. Wang and X. Wang, "A generalized spatial filtering method in broadband active noise control based on independent sound field component analysis," *INTER-NOISE and NOISE-CON Congress and Conference Proceedings*, 2017.

14. S. J. Elliott, "Design and Performance of Feedback Controllers," *Signal Processing for Active Control*, Academic Press, 2001, pp. 271-327.

15. Bhan Lam, Woon-Seng Gan, DongYuan Shi, Masaharu Nishimura, Stephen Elliott, "Ten questions concerning active noise control in the built environment." *Building and Environment*, vol. 200, 107928, 2021.

List of Figure Captions

Fig. 1— Block diagram of the MIMO feedforward ANC controllers using the internal model control structure.

Fig. 2— An intuitive illustration of the modification from original frequency responses of singular vectors to the modified frequency responses that is to be fitted.

Fig. 3—The experimental setup.

Fig. 4—Frequency responses of singular vectors of auto-correlation matrix associated with: (a) the 1st input and 1st output channel, (b) the 2nd input and 1st output channel, (c) the 1st input and 2nd output channel, and (d) the 2nd input and 2nd output channel.

Fig. 5—Comparison of averaged sound pressure at the error microphones for truncated SVD method and proposed singular vector filtering method.

Fig. 6—Comparison of total frequency responses of singular vectors indexed from 120 to 350 for the original response, target response, and filtered response associated with: (a) the 1st input and 1st output channel, (b) the 2nd input and 1st output channel, (c) the 1st input and 2nd output channel, and (d) the 2nd input and 2nd output channel.

Fig. 7—Comparison of averaged sound pressure at the error microphones for regularization method and proposed singular vector filtering method.

Fig. 8— Comparison of averaged sound pressure at the error microphones for two different singular vector filtering methods

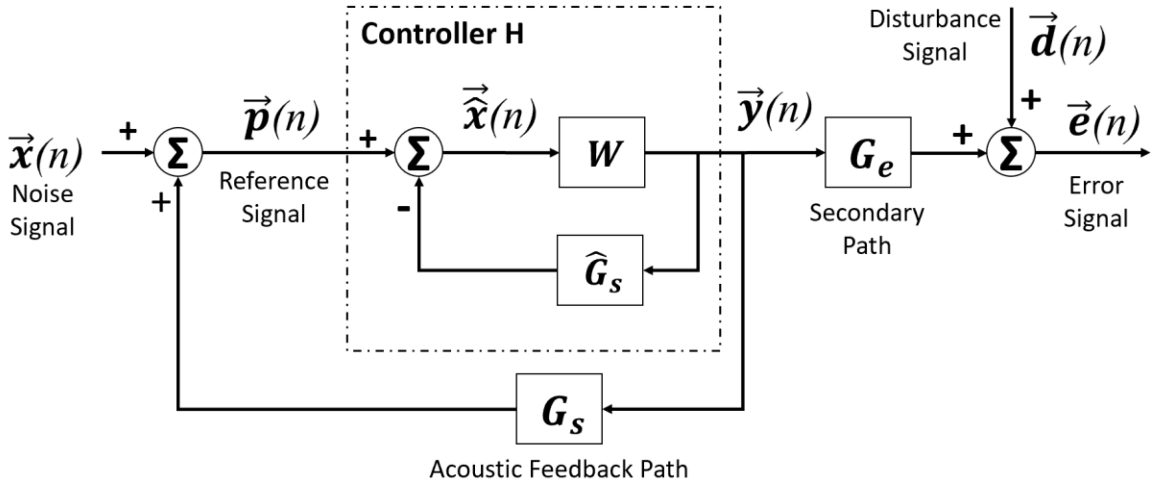

Fig. 1— Block diagram of the MIMO feedforward ANC controllers using the internal model control structure.

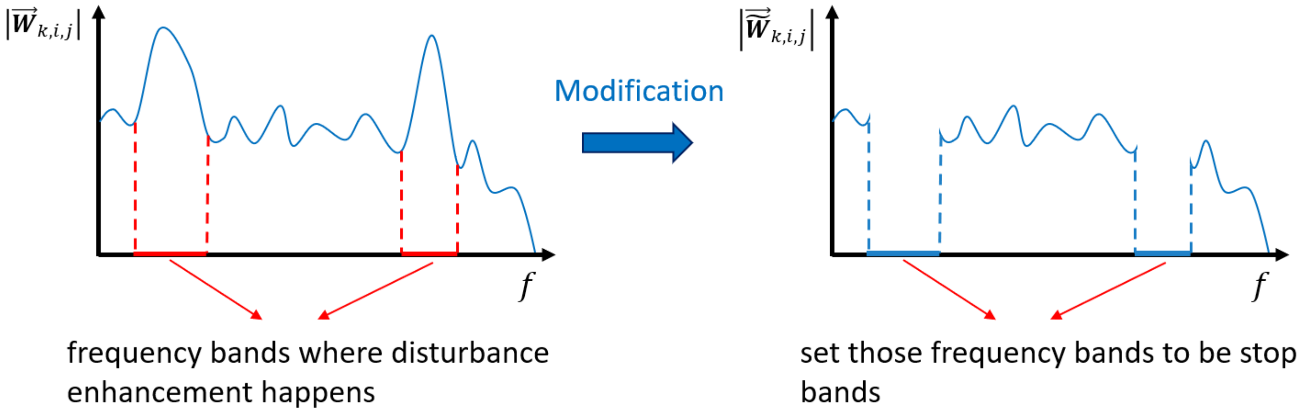

Fig. 2— An intuitive illustration of the modification from original frequency responses of singular vectors to the modified frequency responses that is to be fitted.

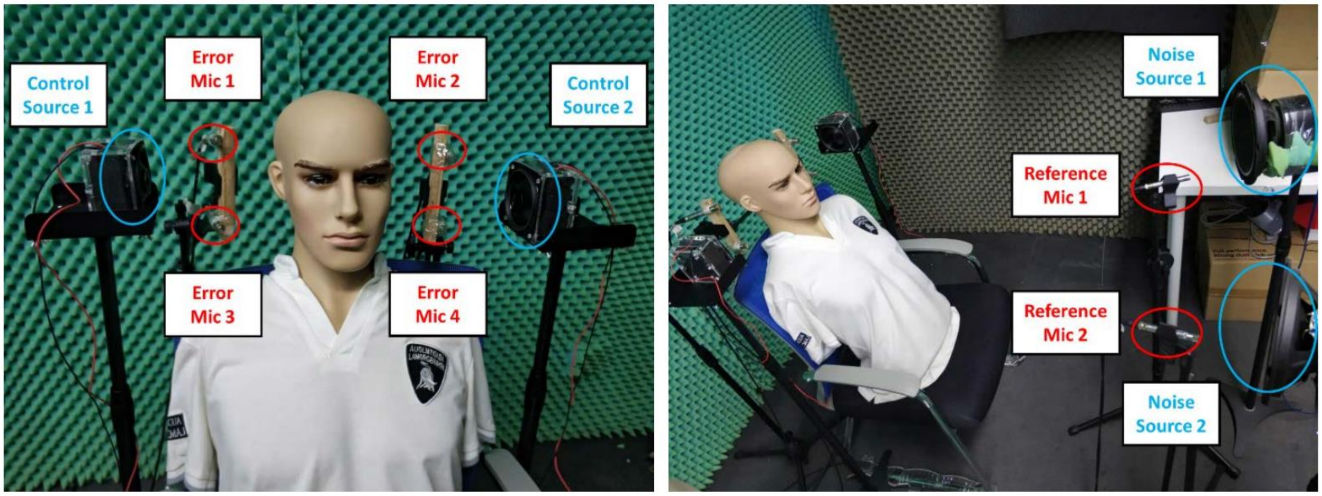

Fig. 3— The experimental setup.

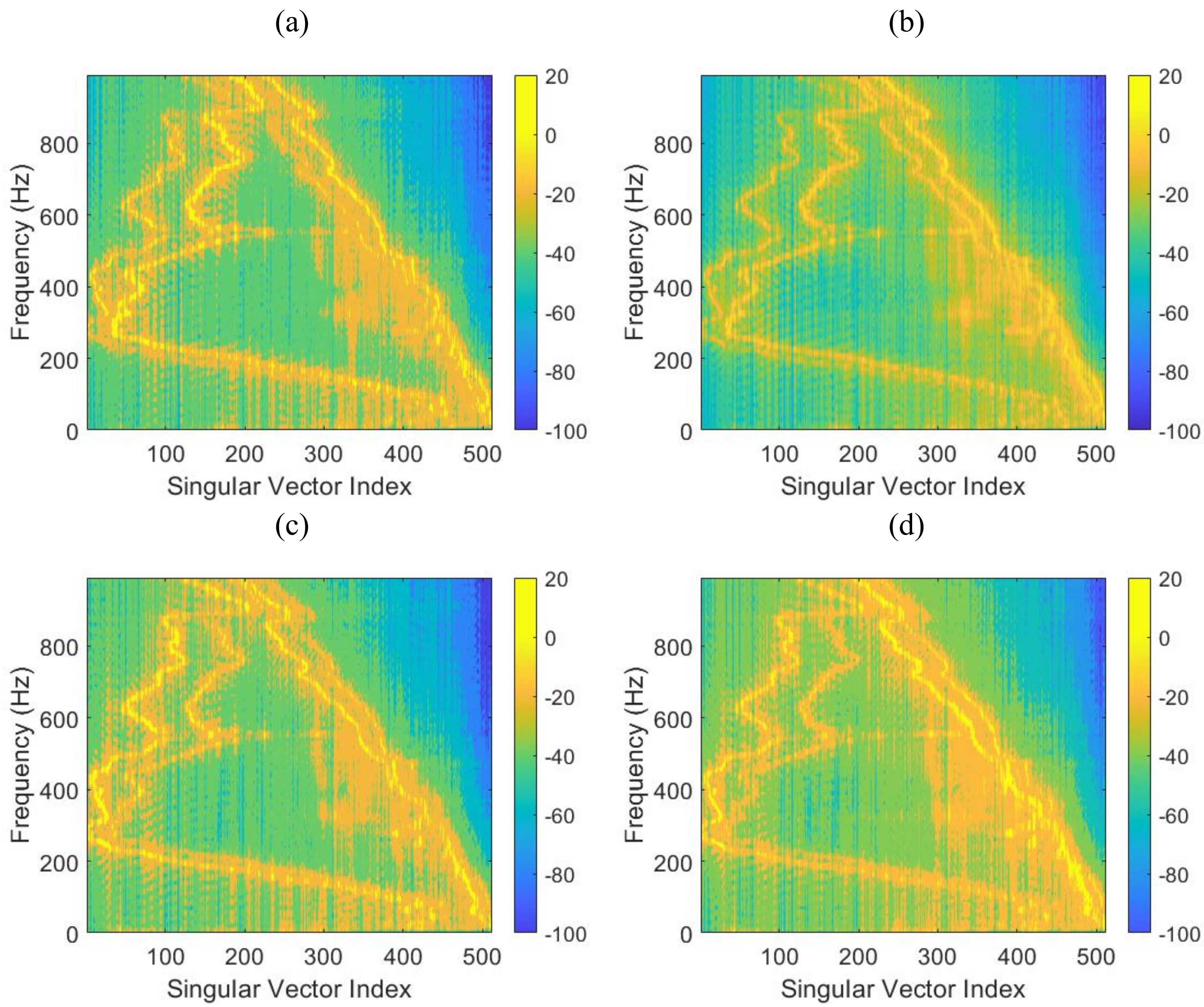

Fig. 4—Frequency responses of singular vectors of auto-correlation matrix associated with: (a) the 1st input and 1st output channel, (b) the 2nd input and 1st output channel, (c) the 1st input and 2nd output channel, and (d) the 2nd input and 2nd output channel.

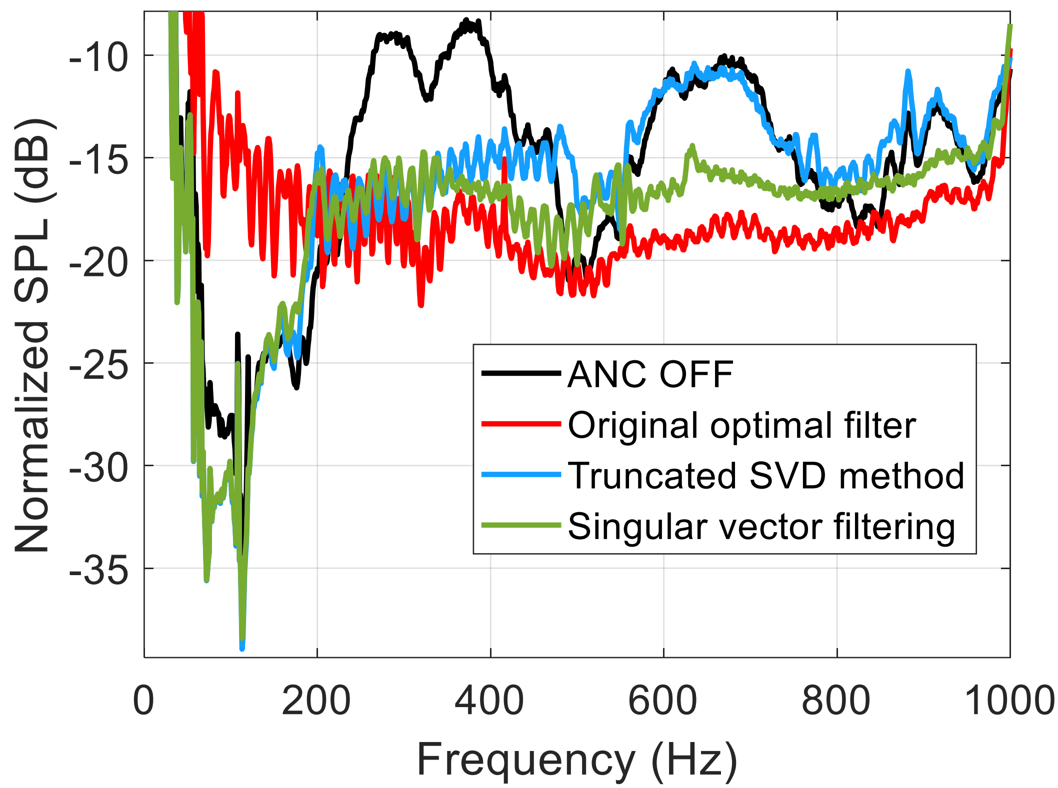

Fig. 5—Comparison of averaged sound pressure at the error microphones for truncated SVD method and proposed singular vector filtering method.

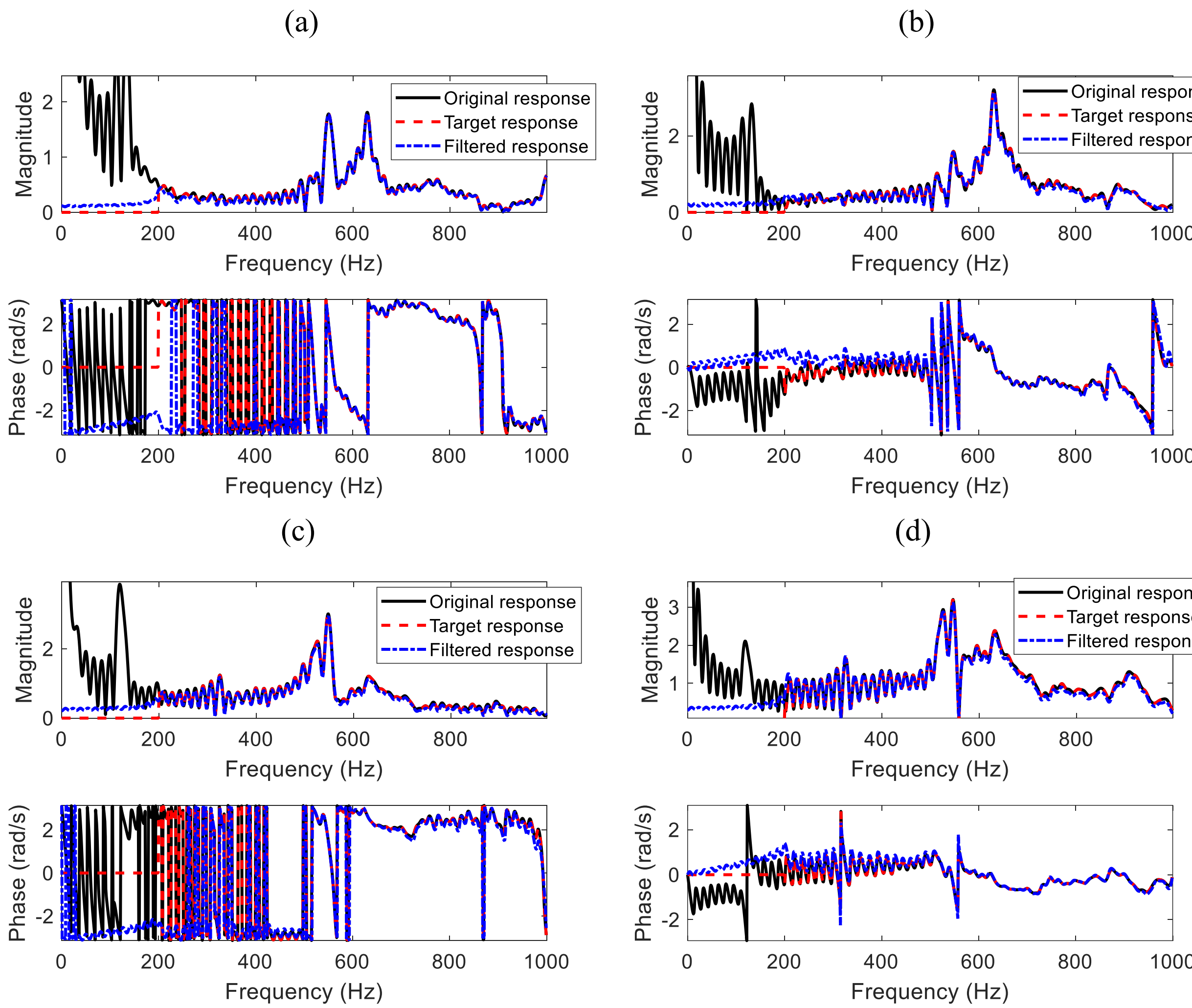

Fig. 6—Comparison of total frequency responses of singular vectors indexed from 120 to 350 for the original response, target response, and filtered response associated with: (a) the 1st input and 1st output channel, (b) the 2nd input and 1st output channel, (c) the 1st input and 2nd output channel, and (d) the 2nd input and 2nd output channel.

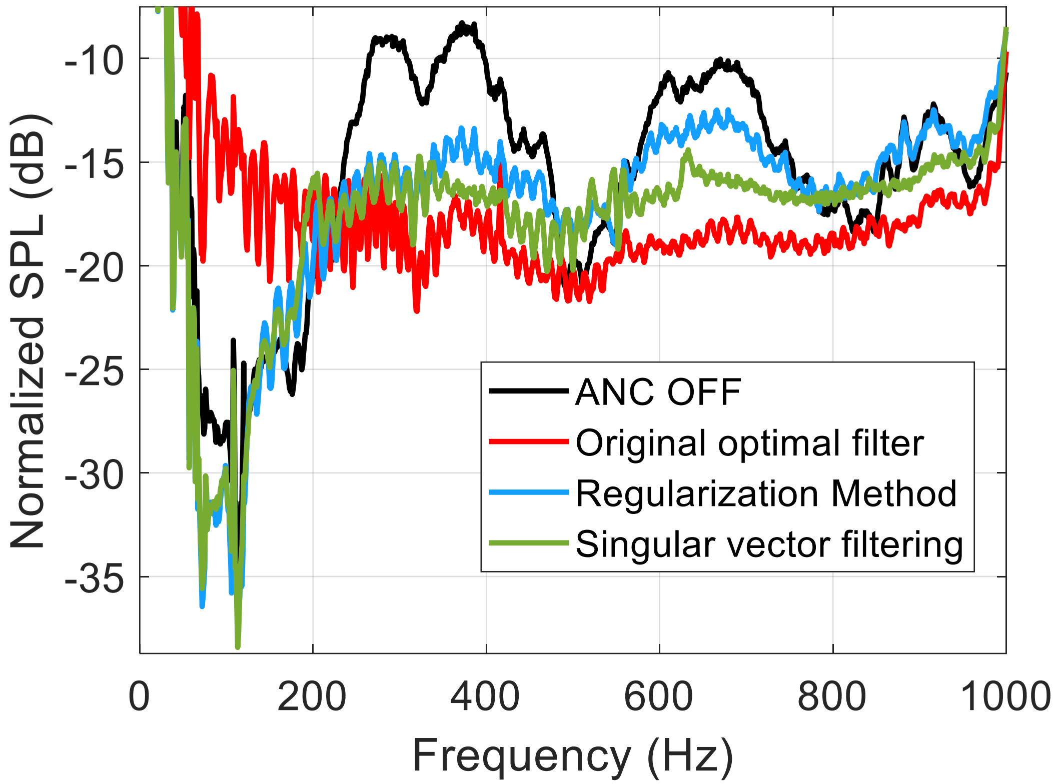

Fig. 7—Comparison of averaged sound pressure at the error microphones for regularization method and proposed singular vector filtering method.

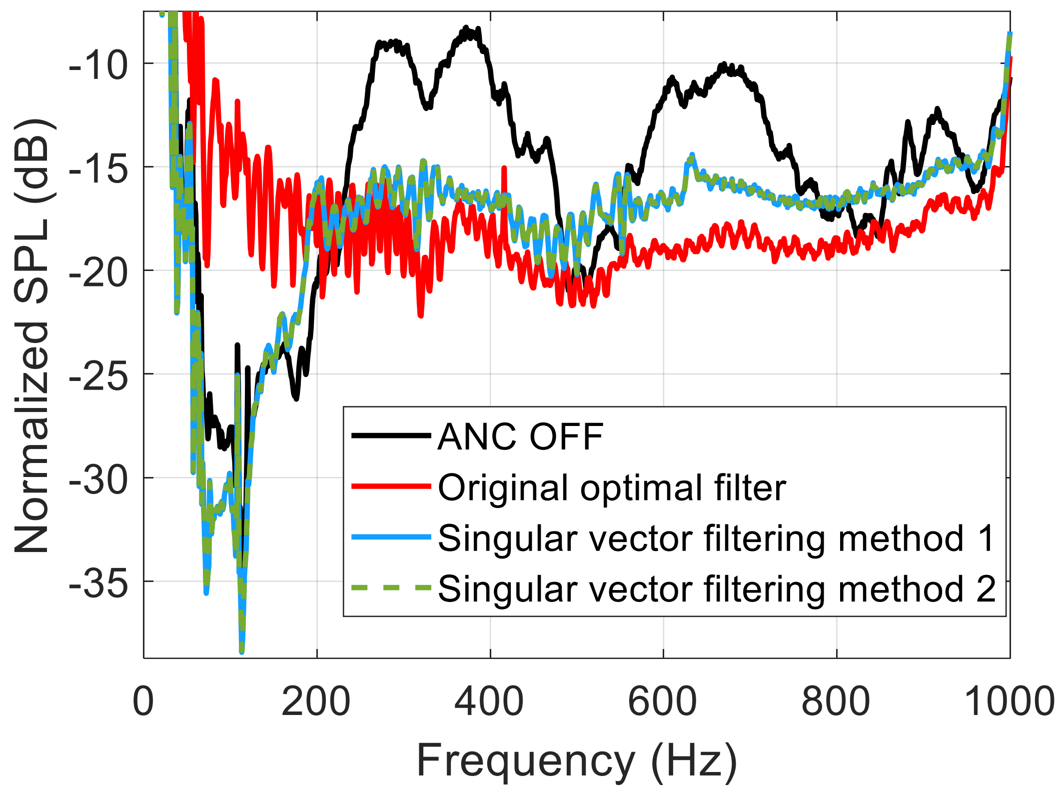

Fig. 8— Comparison of averaged sound pressure at the error microphones for two different singular vector filtering methods